Journal of Materials Processing Technology 159 (2005) 1–8

Journal of Materials Processing Technology

www.elsevier.com/locate/jmatprotec

Effects of over-roll thickness on cone surface roughness in shear spinning

Ming-Der Chen [a], Ray-Quan Hsu [a,*], Kuang-Hua Fuh [b]

[a] *Department of Mechanical Engineering, National Chiao Tung University, 1001 Ta-Hsueh Road, 300 Hsinchu, Taiwan, ROC*
[b] *Department of Mechanical and Marine Engineering, National Taiwan Ocean University, Taiwan, ROC*

Received 12 December 2002; accepted 23 July 2003

Abstract

A high quality of cone surface finish was achieved by carefully controlled over-roll thickness in the shear spinning process. In this study, blank thickness, roller nose radius, mandrel revolution, roller feed and over-roll thickness were taken as major process variables to investigate the effects of the above parameters on the surface roughness of cone shape products. From the experiment, several sets of experimental data were obtained, which in turn were used to construct regression equations for applied forces and product surface roughness. The results were verified by four extra spinning experiments. It is found that deeper over-roll combines with the thinner blank sheet, larger roller nose radius and slower roller feed, and are advantageous for obtaining smoother surface roughness. Over-roll of the blank in shear spinning is an effective way to improve the surface roughness of the product.

Keywords: Shear spinning; Shear force; Surface roughness; Response surface method; Regression analysis; Over-roll thickness

1. Introduction

In shear spinning, a mandrel which was so shaped as to impart the desired contour to the product is attached to a rotating head (lathe chuck), while sheet blank hold by a clamping fixture device, forces it against the mandrel as shown in Fig. 1. While mandrel and blank are rotating, a roller shape forming tool exerts force against the sheet, causing localized plastic deformation. Through the spinning process, blank/roller of contact zone and plastic deformation traverse the blank sheet, completing transformation of mandrel shape onto the blank.

In aerospace applications such as rockets and propulsion units as well as nuclear engineering equipment, surface quality and uniformity of the product thickness are important criteria for selection. Held [1] discovered that in the missile application of the cone inner and exterior surface roughness as well as the type of manufacturing are the essential factors on the jet velocity.

Kalpakcioglu [2] and Kobayashi and Thomsen [3] studied the shear force as a function of a particular process parameter. Zhao and Zhang [4] and Wang et al. [5] described the clearance between roller and mandrel for multi-pass hot spinning. However, the surface finish of spun cones is not an objective of their studies. Besides, interactive influences among these parameters are never considered.

In this article, the authors study the influences of spinning roller radius, mandrel revolution, roller feed, blank thickness and over-roll thickness on the inner and exterior surface roughness in cone spinning. The experiments were conducted at room temperature in a single pass. It is found that in order to obtain good surface qualities and uniform wall thickness, “over-roll”, i.e. thinning of the blank must be applied. When over-roll of the blank is applied, material tends to envelop around the roller nose tip. Thus the contact area of roller and blank in shear spinning (over-roll) is greater than the non-thinning spinning process. Since there are multiple process variables involved in spinning, to investigate the combined influences of these parameters on the cone surface roughness, it is necessary to conduct the experiment analytically. Hence, an experimental design method is adopted, the number of experiments are reduced significantly while the results are still effective. An experimental design matrix is constructed by the Taguchi method. Through regression analysis, a relationship between surface roughness, spinning force and spinning parameters are derived.

* Corresponding author. Tel.: +886-35-712121; fax: +886-35-720634.

0924-0136/$ – see front matter © 2003 Published by Elsevier B.V.
doi:10.1016/j.jmatprotec.2003.07.017

Nomenclature

C_s, x_5	over-roll thickness (mm)
f, x_4	roller feed (mm/rev)
F_p	feeding force Newton (N)
F_t	tangential force Newton (N)
N, x_3	mandrel revolution (rev/min)
R_i	inner surface roughness of part ($\mu m = 10^{-3}$ mm)
R_o	outer surface roughness of part ($\mu m = 10^{-3}$ mm)
t_f	final thickness of cone (mm)
t_0, x_1	original thickness of blank (mm)
Greek letters	
α	half apex angle of mandrel (°)
ρ_R, x_2	roller nose radius (mm)
ψ	roller position angle (°)

2. Experimental design method and procedure

2.1. Experimental design method

The Taguchi method, is a way of designing experimental matrix which are used to find the significance of interactive effects among variables without higher order analysis. On the other hand, the response surface methodology (RSM) [6] which is adopted in the study is a statistical method for establishing relations among process parameters. In this study, the objective of RSM is to build inner, outer surface roughness and spinning force models. Once the experimental results are obtained, the coefficients and variance analysis are then calculated with SAS software to determine the significance of the parameters, and the *T*-test is used to determine which parameters are most significant. The *F*-ratio test is conducted to check the adequacy for the proposed model. Through experiments, surface roughness and spinning force are collected and then fed into a SAS/STAT program to construct statistical regression equations. Blank thickness (x_1), roller nose radius (x_2), mandrel revolutions (x_3), roller feeds (x_4) and over-roll thickness (x_5) were chosen as experimental parameters, each with five levels are shown in Table 1 selected on the basis of preliminary tests. Regression equations for surface roughness models and three shear force components can thus be built. Fig. 2 shows the flow chart of the analysis.

2.2. Experimental devices, materials and procedure

Fig. 1 shows the schematic drawing of a shear spinning device. Spindle power rate is 15 HP, the longitudinal (*Z*-axis) and the latitude (*X*-axis) output are 5 and 3 HP, respectively. The spindle rotates from 100 to 1500 rpm. Forming roller can feed from 0 to 2000 mm/min in *X*-axis and 0 to 3000 mm/min in *Z*-axis. It was constructed from a CNC lathe and a fixture for holding the work-piece was designed to move along with the spinning roller. The mandrel revolutions and roller feeds can be adjusted via CNC controller. The shear spinning processes can be executed through a numerical control program when the mandrel shape and work-piece dimensions are determined. Measuring instruments are listed as follows:

1. Three-channel dynamometer (Kistler 9257A): force output signals were amplified through a three-channel charge amplifier (Kistler 5807A). For the convenience of analy-

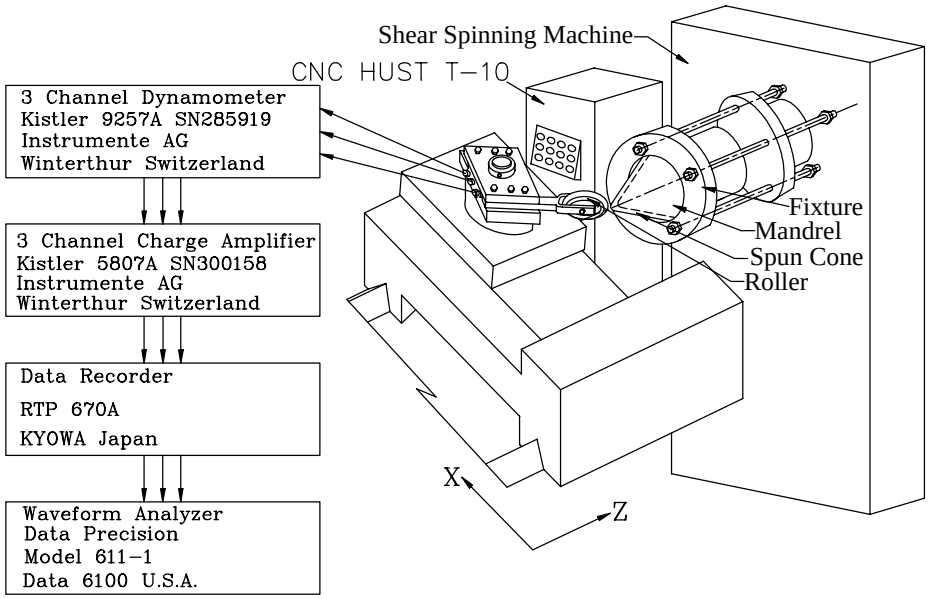

Fig. 1. A schematic diagram of a shear spinning device.

Table 1
Shear spinning parameter combinations

Parameters	Symbols	Levels				
		−2	−1	0	1	2
Blank thickness, t_0 (mm)	x_1	1.5	2.59	4.11	6.0	7.0
Roller nose radius, ρ_R (mm)	x_2	2.5	4.0	4.8	5.5	7.1
Mandrel revolutions, N (rev/min)	x_3	20	40	60	80	90
Roller feeds, f (mm/rev)	x_4	0.10	0.13	0.16	0.18	0.20
Over-roll thickness, C_s (mm)	x_5	0.3	0.4	0.5	0.6	0.7

sis, a data recorder (KYOWA RTP 670A) was connected to the charge amplifier. The recorded data were carefully analyzed through a waveform analyzer (Data Precision Model 6100).
2. Surface roughness measuring equipment (Talysurf 6, Tayler-Hobson).

Blank and tool materials are:

1. Mandrel: Cr–Mo alloys (SAE 4130), hardness of R_c 60–63. Cone angle at the tip of the mandrel is 50° and the nose radius is 5 mm.
2. Forming roller: Cr–Mo alloy (SAE 4130), hardness of R_c 60–63, roller nose radius (2.5, 4.0, 4.8, 5.5 and 7.1 mm).
3. Blank material: A 1100-O aluminum, sheet thickness (1.5, 2.59, 4.11, 6.0 and 7.0 mm).

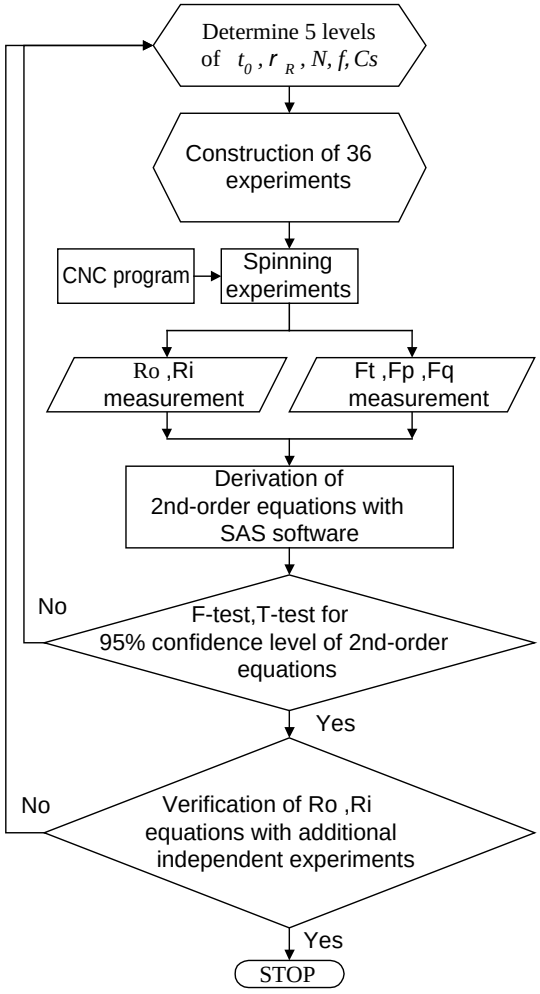

Fig. 2. Flow chart of the analysis.

During the spinning process, the interference of the roller with the blank flange or clamping fixture must be avoided. The roller contact angle ψ, i.e., the angle formed by the roller axis and mandrel axis, is set at 60° throughout the operation as shown in Fig. 3. In addition, thinning of the blank thickness is introduced by setting an over-roll of roller on the blank.

3. Results and discussion

3.1. Results

Table 2 lists the combinations of process parameters in 36 experiments. Experimental results for inner surface roughness R_i, outer surface roughness R_o, tangential force F_t, feeding force F_p and normal force F_q are also recorded in the table. Experimental results were fed into a SAS software package to build a set of second order equations. This process is called regression analysis. Equations thus obtained

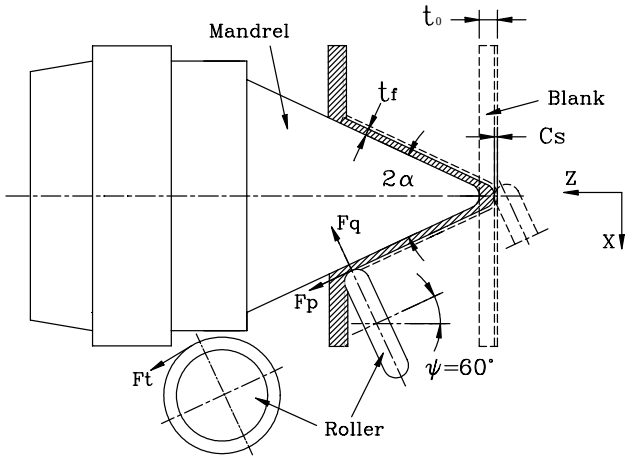

Fig. 3. Three force components and roller contact angle in the shear spinning process.

Table 2
Combinations of spinning parameters and experimental results

	Shear spinning parameters					Experimental results				
	t_0 (mm)	ρ_R (mm)	N (rev/min)	f (mm/rev)	C_s (mm)	R_i[a] (μm)	R_o[a] (m)	F_q (N)	F_p (N)	F_t (N)
1	2.59	4.00	40.00	0.13	0.6	1.08	1.96	962.2	641.4	179.3
2	2.59	5.50	40.00	0.13	0.4	0.96	1.57	983.6	598.9	242.8
3	6.00	4.00	40.00	0.13	0.4	4.6	3.06	1003.9	732.4	293.8
4	6.00	5.50	40.00	0.13	0.6	0.95	2.93	1053.6	779.2	298.9
5	2.59	4.00	40.00	0.18	0.4	1.13	1.65	923.9	579.3	184.2
6	2.59	5.50	40.00	0.18	0.6	1.11	2.06	953.88	623.8	231.6
7	6.00	4.00	40.00	0.18	0.6	1.12	5.49	1031.6	765.4	178.5
8	6.00	5.50	40.00	0.18	0.4	1.84	7.13	1033.7	753.6	206.4
9	2.59	4.00	80.00	0.18	0.6	1.10	2.10	958.3	616.0	207.6
10	2.59	5.50	80.00	0.18	0.4	1.41	2.70	925.9	563.7	225.9
11	6.00	4.00	80.00	0.18	0.4	4.10	6.83	1032.7	738.3	259.3
12	6.00	5.50	80.00	0.18	0.6	2.42	2.33	1086.3	862.9	274.4
13	2.59	4.00	80.00	0.13	0.4	1.04	2.13	995.9	622.5	231.5
14	2.59	5.5	80.00	0.13	0.6	1.02	1.00	923.9	670.9	237.8
15	6.00	4.00	80.00	0.13	0.6	3.87	2.17	1024.0	740.2	281.4
16	6.00	5.50	80.00	0.13	0.4	1.68	2.48	1023.7	772.1	257.9
17	1.50	4.80	60.00	0.16	0.5	1.17	1.54	809.0	410.5	158.3
18	7.00	4.80	60.00	0.16	0.5	4.90	5.66	1058.9	878.2	250.4
19	4.11	2.50	60.00	0.16	0.5	1.01	4.09	968.2	457.1	231.5
20	4.11	7.10	60.00	0.16	0.5	0.84	1.65	980.7	456.9	210.2
21	4.11	4.80	20.00	0.16	0.5	1.01	2.05	1018.3	516.0	203.4
22	4.11	4.80	90.00	0.16	0.5	1.07	3.43	986.9	501.5	232.0
23	4.11	4.80	60.00	0.10	0.5	1.24	2.20	947.8	506.2	231.3
24	4.11	4.80	60.00	0.20	0.5	1.34	4.77	834.9	502.6	231.8
25	4.11	4.80	60.00	0.16	0.3	1.26	2.87	921.9	453.1	221.5
26	4.11	4.80	60.00	0.16	0.7	0.99	1.78	1123.6	827.7	243.5
27	4.11	4.80	60.00	0.16	0.5	1.10	3.37	871.6	494.6	205.1
28	4.11	4.80	60.00	0.16	0.5	1.08	3.38	907.4	520.6	207.3
29	4.11	4.80	60.00	0.16	0.5	0.99	2.19	862.4	514.2	210.9
30	4.11	4.80	60.00	0.16	0.5	1.30	2.51	917.9	509.2	213.7
31	4.11	4.80	60.00	0.16	0.5	1.28	2.75	885.5	505.5	210.0
32	4.11	4.80	60.00	0.16	0.5	1.13	2.19	871.8	510.9	199.2
33	4.11	4.80	60.00	0.16	0.5	1.11	2.32	924.9	510.9	186.9
34	4.11	4.80	60.00	0.16	0.5	1.36	2.59	919.3	520.4	194.5
35	4.11	4.80	60.00	0.16	0.5	0.99	2.62	938.9	506.4	199.4
36	4.11	4.80	60.00	0.16	0.5	1.36	3.25	920.4	511.1	191.8

[a] R_i, R_o; ISO 10 point height parameter. It is the average height difference between the five highest peaks and the five lowest valleys within the sampling length.

are regression equations. These equations depict the correlation among inner, outer surface roughness and spinning force with the process parameters.

Regression equation for inner surface roughness R_i and the process parameters t_0, ρ_R, f, N and C_s takes the following form:

$$\begin{aligned} R_i = {} & 15.58 + 0.25t_0 - 2.04\rho_R - 0.08N - 77.89f \\ & - 6.75C_s + 0.10t_0^2 - 0.04\rho_R^2 - 0.12t_0\rho_R + 0.004t_0N \\ & - 4.86t_0f + 0.36t_0C_s + 21.37\rho_R f - 1.07\rho_R C_s \\ & + 0.11fN + 0.17NC_s \end{aligned} \quad (1)$$

The F-test value for the above equation is 19.62, which is greater than $F_{0.05}(15, 17) = 2.372$. That means Eq. (1) can be accepted within a 95% confidence interval.

Similarly, the outer surface roughness is derived as the following equation:

$$\begin{aligned} R_o = {} & -22.62 + 1.35t_0 + 4.15\rho_R + 0.09N + 36.35C_s \\ & + 201f^2 - 17.75C_s^2 - 0.38t_0\rho_R + 6.04t_0f \\ & - 20.14\rho_R f + 0.5Nf - 0.34NC_s \end{aligned} \quad (2)$$

The F-test value of the equation is 14.56, which is greater than $F_{0.05}(11, 24) = 2.610$. The above equation is acceptable within a 95% confidence level.

The equation for normal force is presented as follows:

$$\begin{aligned} F_q = {} & 3114.82 - 56.74t_0 - 154.83\rho_R - 8.83N - 8676.1f \\ & - 3613.27C_s + 12.95\rho_R^2 + 0.08N^2 + 15551f^2 \\ & + 3013.82C_s^2 + 8.21t_0\rho_R + 303.25t_0f + 5085.72fC_s \end{aligned} \quad (3)$$

Fig. 4. Spun cones from four independent shear spinning experiments.

The T-test value of the above equation indicates the over-roll thickness has a dominant effect on the normal force, i.e. the larger the over-roll thickness, the larger the normal force. F-value is 8.87, which is larger than $F_{0.05}(12, 23) = 2.5175$, the authors ascertained that within a 95% confidence interval, this equation is acceptable.

Feeding force F_p is derived as the following equation:

$$F_p = 3028.17 - 255.28t_0 - 6.39N - 10104f - 5036.54C_s + 27.68t_0^2 + 0.06N^2 + 19414f^2 + 4763C_s^2 + 2.05t_0\rho_R + 405.92t_0 f + 4587.11fC_s \quad (4)$$

The F-test value of Eq. (4) is 11.67, which is larger than $F_{0.05}(11, 24) = 2.610$, it shows that this equation has a 95% confidence level.

The following equation expresses the calculated tangential force F_t along the cone surface:

$$F_t = 1124.88 + 74.14t_0 - 78.01\rho_R - 4.14N - 3827.61f - 1944.07C_s + 3.815\rho_R^2 + 0.024N^2 + 10601f^2 + 906.63C_s^2 - 4.61t_0\rho_R - 252.01t_0 f - 0.549\rho_R N + 194.65\rho_R C_s + 20.07Nf + 2.05NC_s \quad (5)$$

The F-test value of the above equation is 5.839, which is larger than $F_{0.05}(15, 20) = 2.3275$, it shows a 95% confidence level.

In order to check the reliability of the equations induced through regression analysis, independent experiments with process parameters different from the 36 assigned experiments are selected. Fig. 4 presents the spun cones from

Table 3
Comparison of prediction and experimental inner/outer surface roughness at various shear spinning conditions

	t_0 (mm)	ρ_R (mm)	N (rev/min)	f (mm/rev)	C_s (mm)	Prediction, R_i (μm)	Experimental, R_i (μm)	Prediction error (%)	Prediction, R_o (μm)	Experimental, R_o (μm)	Prediction error (%)
1	4.11	4.0	35	0.14	0.5	1.21	1.27	4.96	2.81	3.10	10.32
2	4.11	4.0	55	0.14	0.5	1.33	1.36	2.26	2.61	2.63	0.77
3	2.59	4.0	55	0.11	0.5	1.09	1.11	1.83	1.19	1.18	0.84
4	2.59	4.0	55	0.14	0.5	1.42	1.32	7.04	1.58	1.53	3.16

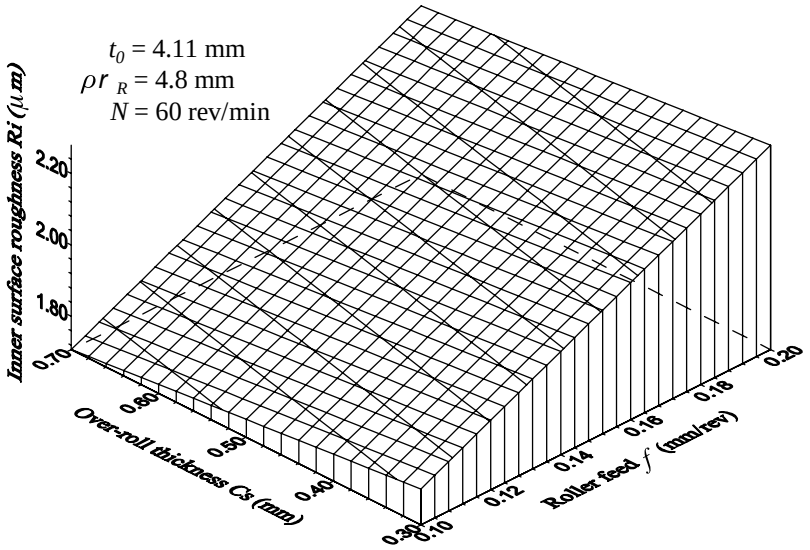

Fig. 5. Effects of roller feed on the inner surface roughness at various over-roll thicknesses.

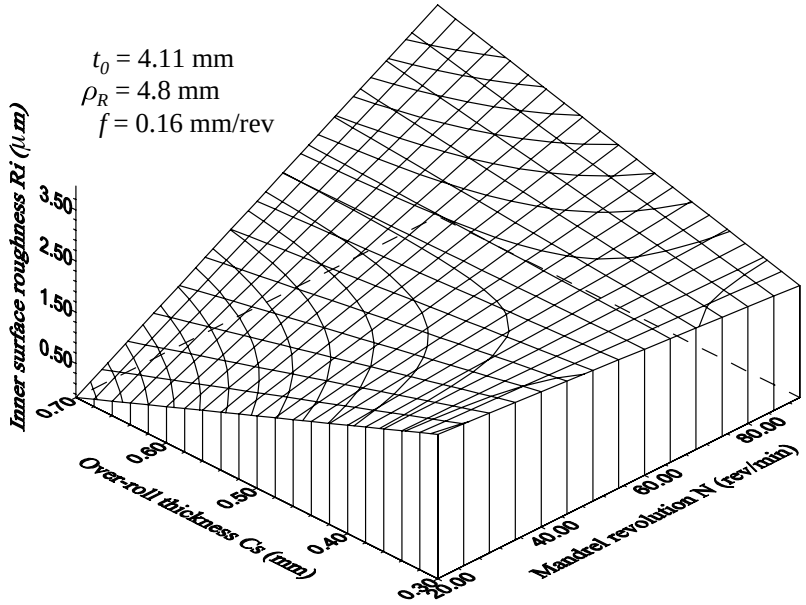

Fig. 6. Effects of mandrel revolution on inner surface roughness at various over-roll thicknesses.

these four independent experiments. Table 3 demonstrates the comparison of the prediction data derived from Eqs. (1) and (2) with the experimental results. From the results, it is found that, the prediction error ranged within 10.4%.

3.2. Discussion

By substituting $t_0 = 4.11$ mm, $\rho_R = 4.8$ mm and $N = 60$ rev/min, Eq. (1) reduces as follows:

$$R_i = 1.41 + 4.75f - 0.25C_s \quad (6)$$

Fig. 5 summarizes the effects of roller feed on inner surface roughness at various over-roll thicknesses. With a fixed roller feed, inner surface roughness decreases with an increasing over-roll thickness. When over-roll thickness is fixed, inner surface roughness decreases with decreasing roller feed. That is, slower roller feed combined with deeper over-roll thickness produces better inner surface roughness of the spun cone. Understandably, with slower roller feed, the rate of deformation of the blank is reduced, it leads to a better inner surface roughness. Furthermore, with deeper over-roll thickness, the blank is much easier to comply with the contour of the mandrel, thus the smoothness of the tool surface is easier to emboss on the blank.

For $t_0 = 4.11$ mm, $\rho_R = 4.8$ mm and $f = 0.16$ mm/rev, Eq. (1) yields to:

$$R_i = 5.97 - 0.06N - 18.45C_s + 0.17NC_s \quad (7)$$

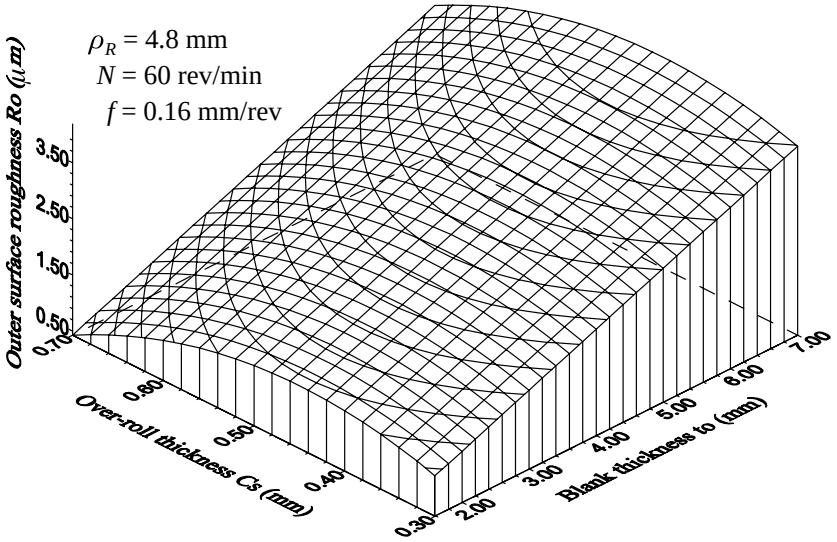

Fig. 7. Effects of blank thickness on the outer surface roughness at various over-roll thicknesses.

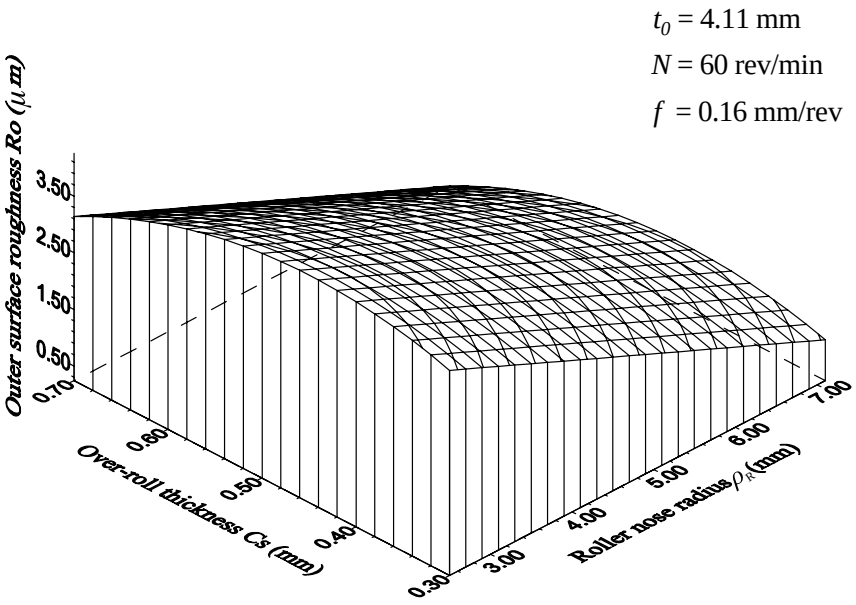

Fig. 8. Effects of roller nose radius on the outer surface roughness at various over-roll thicknesses.

Fig. 6 depicts the mandrel revolution effect on inner surface roughness at various over-roll thicknesses. The finding verifies that regardless of the mandrel revolution, the inner surface roughness decreases with increasing over-roll thickness. The over-roll thickness has an overwhelming effect on the inner surface roughness of the product.

For $\rho_R = 4.8$ mm, $N = 60$ rev/min and $f = 0.16$ mm/rev, Eq. (2) becomes:

$$R_o = -2.82 + 0.49t_0 + 15.95C_s - 17.75C_s^2 \quad (8)$$

From Eq. (8), the effect of the blank thickness on the outer surface roughness at distinct over-roll thicknesses is obtained. The result is shown in Fig. 7. The configuration reveals that with a fixed over-roll thickness, outer surface roughness becomes smaller with a decreasing blank thickness. At a fixed blank thickness, the outer surface roughness increases with decreasing over-roll thickness, then reaches a maximum at about $C_s = 0.45$ mm. Beyond this value, the outer surface roughness decreases with decreasing over-roll thickness. Reasonably, the thicker the blank, the more energy is required for the material to deform and then smoothness of the surface of cones cannot be achieved as easy as a thinner blank. Besides, blank thickness has a much more significant effect on the outer surface roughness.

For $t_0 = 4.11$ mm, $N = 60$ rev/min and $f = 0.16$ mm/rev, Eq. (2) simplifies to:

$$R_o = 2.25 - 0.63\rho_R + 15.95C_s - 17.75C_s^2 \quad (9)$$

Fig. 8 shows the effects of roller nose radius on the outer surface roughness at various over-roll thicknesses. The configuration confirms that as the roller nose radius increases, the outer surface roughness decreases in size. Because the outer surface of the blank is in direct contact with the roller, a larger roller nose radius implies a larger contact area, thus producing a smoother deformation of the material. On the other hand, with a fixed roller nose radius, the outer surface roughness is increasing along with decreasing over-roll thickness. At approximately $C_s = 0.5$ mm, outer surface roughness reaches a maximum. For over-roll thickness thinner than this value, the outer surface roughness decreases with decreasing over-roll thickness.

4. Conclusions

In this study, the following conclusions are drawn:

1. Single pass spinning processes at room temperature, can be significantly improved with proper choice of over-roll thickness.
2. The inner/outer surface roughness and the shear force equations in relation to blank thickness, roller nose radius, mandrel revolution, roller feed and over-roll thickness are derived from experimental data with the help of regression analysis.
3. The analytic data show that these equations are acceptable within a 95% confidence interval.
4. Results obtained from the regression equations, agree well with the experiments.

References

[1] M. Held, Determination of the material quality of copper shaped charge liners, Propell. Explos. Pyrot. 10 (1985) 125–128.
[2] S. Kalpakcioglu, A study of shear-spinnability of metals, Trans. ASME, J. Eng. Ind. 83 (1961) 478–484.

[3] S. Kobayashi, E.G. Thomsen, A theory of shear spinning of cones, Trans. ASME, J. Eng. Ind. (1961) 485–495.
[4] Y. Zhao, S. Zhang, The shear spinning of flanged container head, in: Proceedings of the Fourth International Conference on Technology of Plasticity, 1993, pp. 1436–1438.
[5] D. Wang, X. Cheng, W. Wan, Spinning forming technique and quality of 30 CrMnSiA high precision end, in: Proceedings of the Fourth International Conference on Technology of Plasticity, 1993, pp. 1448–1452.
[6] G.E.P. Box, W.G. Hunter, J.S. Hunter, Statistics for Experiments: An Introduction to Design, Data Analysis and Model Building, Wiley, New York, 1978.